Influence of nonlinear detuning at plasma wavebreaking threshold on backward Raman compression of non-relativistic laser pulses

A. A. Balakin,[1] G. M. Fraiman,[1] Q. Jia,[2] and N. J. Fisch[2]
[1]*Institute of Applied Physics RAS, Nizhny Novgorod 603950, Russia*
[2]*Princeton University, Princeton, New Jersey 08544, USA*

(Received 12 March 2018; accepted 18 May 2018; published online 5 June 2018)

Taking into account the nonlinear dispersion of the plasma wave, the fluid equations for the three-wave (Raman) interaction in plasmas are derived. It is found that, in some parameter regimes, the nonlinear detuning resulting from the plasma wave dispersion during Raman compression limits the plasma wave amplitude to noticeably below the generally recognized wavebreaking threshold. Particle-in-cell simulations confirm the theoretical estimates. For weakly nonlinear dispersion, the detuning effect can be counteracted by pump chirping or, equivalently, by upshifting slightly the pump frequency, so that the frequency-upshifted pump interacts with the seed at the point where the plasma wave enters the nonlinear stage. *Published by AIP Publishing.*
https://doi.org/10.1063/1.5028567

I. INTRODUCTION

In developing the next generation of ultra-high power (exawatt and even beyond) laser systems, the current state-of-art technique of chirped pulse amplification (CPA) is challenged by the low tolerable intensity threshold of its optimal gratings. Stimulated Raman backward scattering (SRBS) in plasmas has been suggested as a promising amplification method to overcome this constraint to achieve intensities 10^4–10^5 times larger than the CPA.[1] The SRBS methodology is based on a resonant three-wave interaction, where a moderately intense, long pump beam (with carrier frequency ω_0) transfers its energy to a counter propagating short seed pulse (at frequency ω_b) through a Langmuir oscillation, which is excited at the plasma frequency ($\omega_p = \omega_0 - \omega_b$) by the resonant beating of the two beams. During the nonlinear stage of the SRBS, where the pump beam is highly depleted, the seed front grows together with self-contraction, resulting in a self-similar amplified seed pulse with a peak intensity much higher than that of the pump. This process is known as Raman compression, which has been extensively studied theoretically[2,3] and demonstrated experimentally.[4–9]

The ideal energy conversion efficiency of the decay is ω_b/ω_0 if each pump photon is converted into a counter-propagating photon. However, several processes can limit the efficiency.

First, there are deleterious processes that affect the lasers, such as the decay of the pump before it reaches the seed,[10] the formation of precursors that interfere with the mediation of the plasma wave,[11] or the forward scattering of the seed pulse.[12] The seed pulse also becomes very intense, making it subject to filamentation instabilities.[13–16] These deleterious processes are often avoided by frequency chirping the pump, together with imposing density gradients in the plasma to compensate for the detuning,[17] or chirping the seed lasers to compensate for group velocity dispersion,[18] or other ways of making use of the bandwidth of the pump or chirping.[19–24] This compensation, namely, that chirping the pump could compensate detuning due to density gradients, thereby facilitating the Raman amplification, was demonstrated experimentally.[9,25,26]

Second, there are processes that affect the mediating Langmuir wave, such as collisional damping or wavebreaking. The collisional damping occurs in high-density, low-temperature regimes and is prone to affect the Langmuir wave more than the laser pump or seed because of the lower frequency of the former. The wavebreaking limits the efficiency,[27–29] making the Raman amplification in lower density plasmas less efficient that otherwise might have been more efficient.[30] The deleterious effects of both the wavebreaking and the collisional damping of the Langmuir wave can be mitigated, in part, by arranging for a high intensity seed pulse, leading to a quasi-transient regime, where the intense seed pulse depletes the pump before the Langmuir wave is extinguished.[31,32] The front of the seed pulse is then amplified and compressed, with the secondary spikes of the characteristic π-pulse solution being absent.

Our interest here is in processes that affect the mediating Langmuir wave. In order for wavebreaking to occur, the Langmuir wave is necessarily intense, which means that its frequency is subject to detuning nonlinear in its amplitude. However, the nonlinear detuning could also interfere with the mediation of the Raman compression effect, which requires resonance. In fact, as we show here, there are regimes in which the detuning effect caused by the nonlinear dispersion of the plasma wave interferes with the Raman compression at plasma wave amplitude lower than the wavebreaking threshold. We also show that the deleterious effects of the detuning can be dealt with similarly by moderate pump chirping or upshifting the pump frequency in the nonlinear regime.

Note that, in the regime contemplated where detuning effects occur before wavebreaking happens, the fluid equations should provide an adequate description since kinetic effects can then be ignored. Other electron heating effects, such as Landau damping, will be also negligible for quasi-monochromatic pulses, with duration larger than the plasma

period, as contemplated here. The electron dynamics are then regular and periodic, so that the electron heating is negligible. With electron heating being negligible, the plasma need not to be modeled kinetically.

Wavebreaking, besides interfering with the resonant interaction, also introduces kinetic effects. The breakup of the Langmuir wave occurs when the electron longitudinal quiver velocity $v_{\rm osc}$ exceeds the phase velocity $v_{\rm ph} \simeq \frac{c}{2}\,\omega_p/\omega_0$ of the plasma wave. In the limit in which the pump is depleted, namely, the high-efficiency regime of Raman compression, the amplitude of the Langmuir oscillations is determined by the pump intensity, so that wavebreaking threshold can be written as a function of the pump amplitude[1] as

$$a_0 \geq a_{\rm br} \equiv \left(\frac{\omega_p}{2\omega_0}\right)^{3/2}, \tag{1}$$

where $a_0 = eA_0/mc$ is the normalized vector-potential for the pump pulse. The conversion efficiency is maximum when the pump amplitude is a little below the wavebreaking threshold [Eq. (1)] since the efficiency drops drastically with increasing pump amplitude in the wavebreaking regime, as predicted analytically[1] and demonstrated numerically.[27,28]

However, some care should be taken when considering the nonlinear plasma response for large enough pump amplitudes. The nonlinear response introduces a nonlinear phase shift for the plasma wave, which effectively detunes the three-wave resonance conditions. It is shown here that it may stop Raman amplification even before the plasma wavebreaking. In the following basic formulas for this new plasma, nonlinear detuning effects are derived and solved numerically together with particle-in-cell (PIC) simulation verification. To counteract this nonlinear detuning by plasma wave dispersion, it is partially effective to chirp the pump laser or upshift the pump frequency in the nonlinear stage.

This paper is organized as follows: In Sec. II, we derive the nonlinear fluid equations. In Sec. III, we identify regimes wherein the detuning dominates. In Sec. IV, we present numerical simulations, including PIC simulations that model kinetic effects, to verify the analytical predictions. In Sec. V, we summarize our conclusions.

II. FLUID EQUATIONS

The wave equations of the wave packets propagating along the z-axis with the normalized total vector potential $a_\Sigma = \frac{e}{mc}(A_x + \mathrm{i}A_y)$ for pump and seed pulses have the form

$$\frac{\partial^2 a_\Sigma}{\partial t^2} - \Delta_\perp a_\Sigma - \frac{\partial^2 a_\Sigma}{\partial z^2} = -j_\perp = -\beta n a_\Sigma, \tag{2}$$

where $\beta = \omega_p^2/\omega_0^2 = 4\pi N e^2/m\omega_0^2$, n is the plasma density normalized by the initial electron density N, $\Delta_\perp = \partial_{xx} + \partial_{yy}$ is the transverse Laplacian, and $j_\perp = \beta n a_\Sigma$ is the transverse current caused by electron motion for given vector potential. The spatial coordinates and time are normalized by the wavevector and the laser frequency respectively: $t = \omega_0 t_{\rm old}$ and $z = z_{\rm old}\omega_0/c$.

Using the quasi-one-dimensional hydrodynamic approximation for a laser pulse much wider than the plasma period, c/ω_p, the plasma response can be described by

$$\frac{\partial n}{\partial t} + \frac{\partial nv}{\partial z} = 0, \tag{3a}$$

$$\frac{\partial v}{\partial t} = \frac{\partial}{\partial z}\left(\phi - Tn - \frac{v^2}{2} - \frac{|a_\Sigma|^2}{2}\right), \tag{3b}$$

$$\frac{\partial^2 \phi}{\partial z^2} = \beta(n-1). \tag{3c}$$

Here, v is the electron velocity normalized to the speed of light c, $T = 3v_{\rm Te}^2/c^2$ is the normalized electron temperature, and $\phi = e\Phi/mc^2$ is the normalized scalar potential.

For counter-propagating laser pulses, the overall vector potential can be written in the form $a^\Sigma = a\mathrm{e}^{\mathrm{i}(t+z)} + b\mathrm{e}^{\mathrm{i}(t-z)}$, where a and b are the envelope amplitudes of the pump wave (which propagates in the negative z direction) and the seed wave (which propagates in the positive z direction), respectively. The envelope approximation holds for laser intensities smooth enough compared to the wavelength scale, namely,

$$|\partial_t a|, |\partial_z a| \ll |a| \ll 1, \quad |\partial_t b|, |\partial_z b| \ll |b| \ll 1.$$

In this configuration, the plasma response is a beat-wave, with spatial modulation proportional to $\mathrm{e}^{2\mathrm{i}z}$. Thus, the electron density and velocity could be written as the composition of the averaged terms rapidly varying in space

$$\begin{aligned} n &= 1 + (f\mathrm{e}^{2\mathrm{i}z} + f_2\mathrm{e}^{4\mathrm{i}z} + c.c.), \\ v &= \delta v + (q\mathrm{e}^{2\mathrm{i}z} + q_2\mathrm{e}^{4\mathrm{i}z} + c.c.). \end{aligned} \tag{4}$$

Here, the amplitude of the beat-wave is assumed to be small, i.e., $|f|, |q|, |f_2|, |q_2| \propto |a| \ll 1$. Essentially, wavebreaking is caused by the nonlinear term $\partial_z(v^2/2) = v\partial_z v$, which is a kind of quadratic nonlinearity as f^2, $q^2 \ll 1$. Since the quadratic nonlinearities make no contribution to the resonant response in the first order analysis of perturbation theory, here we particularly keep the second order beat-waves (terms proportional to $\mathrm{e}^{4\mathrm{i}z}$) to make the second order perturbation analysis.

Note that the effect on the density of quasi-static terms (such as intensity $|a|^2$ or averaged current $fq^* + qf^*$) will be exponentially small [proportional to $\gamma/\omega_p \exp(-\omega_p/\gamma) \ll 1$] in the parameter region of interest for three-wave decay. The smallness of these effects arises from the smoothness of all pulse envelopes on the scale of the plasma period and the smallness of their amplitudes in comparison to relativistic ones. However, to satisfy Eq. (3a), the nonzero quasi-static velocity δv introduced in Eq. (4) can be put as

$$\delta v = -(fq^* + qf^*). \tag{5}$$

Let us analyze equations for the rapidly oscillating plasma response. First of all, inserting the plasma density response, Eq. (4), into the Poisson equation, Eq. (3c), the scalar potential expression is obtained as

$$\phi \approx -\frac{\beta}{4} f e^{2iz} - \frac{\beta}{16} f_2 e^{4iz} + c.c. \tag{6}$$

Using the same procedure, inserting (4) into Eq. (3a) and Eq. (3b), the equations for the second order terms f_2 and q_2 are obtained as the form of a linear oscillator

$$i\frac{\partial f_2}{\partial t} = 4q_2 + 4fq, \quad i\frac{\partial q_2}{\partial t} = \left(\frac{\beta}{4} + 4T\right) f_2 + 2q^2,$$

with eigenfrequency $\sqrt{\beta + 16T}$ under the "external force" $4fq, 2q^2 \propto e^{2i\omega_f t}$ at frequency $2\omega_f$. Here, $\omega_f = \sqrt{\beta + 4T}$ is the frequency of the plasma wave. Since the solutions for f_2 and q_2 have to be of the same frequency, i.e., $f_2, q_2 \propto e^{2i\omega_f t}$, the non-resonant frequency; We can replace $\partial/\partial t \to 2i\omega_f$ for the quasi-monochromatic plasma response. Thus, the algebraic equations for f_2 and q_2 are

$$\begin{aligned} -2\omega_f f_2 &= 4q_2 + 4fq, \\ -2\omega_f q_2 &= \frac{\beta + 16T}{4} f_2 + 2q^2, \end{aligned}$$

with the following solutions:

$$f_2 = \frac{8q^2}{3\beta} - \frac{8fq\omega_f}{3\beta}, \tag{7a}$$

$$q_2 = \frac{\beta + 16T}{3\beta} fq - \frac{4\omega_f}{3\beta} q^2. \tag{7b}$$

Combining Eqs. (3)–(7), we then can derive the equations for first order plasma response f, q

$$i\dot{q} = \frac{\omega_f^2}{2} f + ab^* - 2f^* q^2 - \frac{4\beta - 32T}{3\beta} |q|^2 f - \frac{8\omega_f}{3\beta} |q|^2 q, \tag{8a}$$

$$\begin{aligned} i\dot{f} = {} & 2q + \frac{16}{3\beta} |q|^2 q - \frac{4\beta - 32T}{3\beta} |f|^2 q - 2f^2 q^* \\ & - \frac{8\omega_f}{3\beta} (2|q|^2 f + f^* q^2). \end{aligned} \tag{8b}$$

Here, we emphasize that the nonlinear terms are responsible for nonlinear detuning of plasma wave approaching wavebreaking. These nonlinear terms are retained despite their seemingly smallness (proportional to $|a|^3$ due to $|f|, |q|, |b| \propto |a| \ll 1$) compared to the Raman term ($ab^* \propto |a|^2$) since these terms are inversely proportional to another small parameter $\beta \ll 1$. It turns out [see Eq. (25)] that for rather rare plasma $\beta^{5/4} \leq |a|$, the magnitude of these nonlinear detuning terms can be the same order as the Raman term ab^*.

Equation (8) is in the form of equations for a complex-valued nonlinear oscillator with eigenfrequencies $\pm\omega_f$. There are two kinds of solutions: one with positive eigenfrequency $f, q \propto e^{+i\omega_f t}$ and the other with negative eigenfrequency $f, q \propto e^{-i\omega_f t}$. This can be seen immediately if we rewrite Eq. (8) for quantities $q \pm \omega_f f/2$. Note that the "external force" has only positive frequency ($ab^* \propto e^{+i\omega_f t}$), which corresponds to the redshift of 3-wave coupling. As result, one of the equations

$$\begin{aligned} i\partial_t \left(q + \frac{\omega_f}{2} f\right) = {} & \omega_f \left(q + \frac{\omega_f}{2} f\right) + ab^* - 4|q|^2 f \\ & - \frac{10}{3} q^2 f^* - \omega_f f^2 q^* - \frac{2\omega_f}{3} |f|^2 q \\ & - \frac{16T}{3\beta} \left(q^2 f^* - \omega_f |f|^2 q\right) \end{aligned}$$

becomes algebraic and leads to the relationship between f and q

$$q + \frac{\omega_f}{2} f \approx -\frac{ab^*}{2\omega_f}. \tag{9}$$

Substituting this relationship into the equation for $q - \omega_f f/2$

$$\begin{aligned} i\partial_t \left(q - \frac{\omega_f}{2} f\right) = {} & -\omega_f \left(q - \frac{\omega_f}{2} f\right) + ab^* - \frac{2}{3} q^2 f^* \\ & + \frac{4}{3} |q|^2 f + \omega_f f^2 q^* + \frac{2\omega_f}{3} |f|^2 q - \frac{16\omega_f}{3\beta} |q|^2 q \\ & + \frac{16T}{3\beta} \left(4|q|^2 f + q^2 f^* - \omega_f |f|^2 q\right) \end{aligned}$$

and using the smallness $|ab^*| \ll \sqrt{\beta}|f|$ and smoothness of external force ab^*

$$\dot{q} \approx -\frac{\omega_f}{2} \dot{f} - \frac{iab^*}{2},$$

we obtain the equation for plasma wave f

$$\frac{\partial f}{\partial t} = i\omega_f f + \frac{i}{\omega_f} ab^* + i\frac{12T\omega_f}{\beta} |f|^2 f. \tag{10}$$

A similar equation was employed in Refs. 33–35.

The equations for laser pulses a and b are obtained straightforwardly by keeping the first nonzero derivative on the envelope equations [Eq. (2)]

$$\frac{\partial a}{\partial t} - \frac{\partial a}{\partial z} = \frac{i\beta}{2} (a + bf) - \frac{i}{2} \Delta_\perp a, \tag{11}$$

$$\frac{\partial b}{\partial t} + \frac{\partial b}{\partial z} = \frac{i\beta}{2} (b + af^*) - \frac{i}{2} \Delta_\perp b. \tag{12}$$

By introducing the dimensionless time $\tau = \gamma t \equiv t a_0 \sqrt{\omega_f/2}$ ($\gamma = a_0\sqrt{\omega_f/2}$ is the linear Raman growth rate) and amplitudes for the pump $a = a_0 \bar{a} e^{-i\beta t/2}$, seed $b = a_0 \bar{b} e^{-i\beta t/2 - i\omega_f (t-z)}$, and for plasma wave $f = i\sqrt{2} a_0 \bar{f} e^{i\omega_f t}/\omega_f^{3/2}$, Eqs. (10)–(12) can be rewritten in the traditional form of 3-wave Raman coupling equations

$$\frac{\partial \bar{a}}{\partial \tau} - \frac{\partial \bar{a}}{\partial z} = -\bar{b}\bar{f}, \tag{13a}$$

$$\frac{\partial \bar{b}}{\partial \tau} + \frac{\partial \bar{b}}{\partial z} = \bar{a}\bar{f}^*, \tag{13b}$$

$$\frac{\partial \bar{f}}{\partial \tau} = \bar{a}\bar{b}^* + iB|\bar{f}|^2 \bar{f}. \tag{13c}$$

Here, $B = 24\sqrt{2} T a_0/\beta\omega_f^{5/2}$. Thus, we obtain the new cubic nonlinearity term $iB|\bar{f}|^2\bar{f}$—the nonlinear detuning results

from the nonlinear dispersion. Then, we will analyze its effects on Raman amplification.

III. IDENTIFICATION OF REGIMES

From Eq. (13c), we can see that including the cubic nonlinear term basically introduces a nonlinear frequency shift ($B|\bar{f}|^2$) to the plasma wave, which detunes the three-wave coupling process. In the following, we roughly estimate this detuning effect on the final maximum amplitude of the output seed and the compression efficiency.

In the nonlinear stage of Raman amplification, the plasma wave amplitude f is almost constant. It is thus reasonable to expect it to be continuously constant as the plasma wave amplitude approaches the wavebreaking regime. This constant plasma wave amplitude assumption $f \approx f_{\max}$ now facilitates the estimation of output seed pulse properties.

In particular, the maximal seed amplitude $b_{\max}$ can be estimated from Eq. (12), which for constant $f = f_{\max}$ takes the form

$$\dot{b} \propto \frac{\beta}{2} a_0 f_{\max} \;\Rightarrow\; b_{\max} \propto \beta a_0 f_{\max} L = \beta^{3/4} f_{\max} \Delta. \tag{14}$$

Here, $\Delta = \gamma L$, L is the interaction length in the nonlinear stage. Since the leading edge of the seed is not influenced by plasma wave saturation, the final seed pulse duration should be the same as that in π-pulse solution,[2] i.e.,

$$\tau \propto \frac{1}{L\gamma^2} \propto \frac{1}{La_0^2\sqrt{\beta}}. \tag{15}$$

Thus, the compression efficiency η, namely, the ratio of output seed energy to the input pump energy, is estimated as

$$\eta = \frac{1}{La_0^2} \int |b|^2 dt \approx \frac{b_{\max}^2 \tau}{La_0^2} \propto \frac{\beta^{3/2} f_{\max}^2}{a_0^2}. \tag{16}$$

Now note that, for the well-known ideal π-pulse solution,[1] the amplitude of the plasma wave at the highly developed, nonlinear stage ($b_{\max} > a_0$) can be put as

$$\omega_p \gamma f_{\max} \simeq a_0^2 \quad \Rightarrow \quad f_{\max}^{\pi} \approx \frac{a_0}{\beta^{3/4}}. \tag{17}$$

Inserting Eq. (17) into Eqs. (14) and (16), the maximum output seed amplitude and compression efficiency in the π-pulse regime are estimated as

$$b_{\max}^{\pi} \propto \beta^{1/4} a_0^2 L = a_0 \Delta, \quad \eta^{\pi} = \text{const}, \tag{18}$$

which agrees with the exact analytical solution.

We now apply these formulas to the classical wavebreaking regime,[2] where the electron quiver velocity in the plasma wave exceeds the plasma wave phase velocity. Taking into account the relation equation (9), this condition can be rewritten as

$$v_{\text{osc}} = |q| = \left| \frac{\sqrt{\beta}}{2} f \right| \geq v_{\text{ph}} = \frac{\omega_p}{2k_0 c} = \frac{\sqrt{\beta}}{2} \;\Rightarrow\; f_{\max}^{\text{wb}} = 1. \tag{19}$$

Thus, it is demonstrated that the wavebreaking occurs only when density perturbations exceed the background plasma density. It is obvious that the approximation equation (4) becomes inapplicable for such large perturbations and the fluid model [(10)–(13)] also becomes invalid. Again, inserting Eq. (19) into Eqs. (14) and (16), the maximum amplitude and efficiency in the classical wavebreaking regime are estimated as

$$b_{\max}^{\text{wb}} \propto \beta a_0 L = \beta^{3/4} \Delta, \quad \eta^{\text{wb}} \propto \frac{\beta^{3/2}}{a_0^2}, \tag{20}$$

i.e., the efficiency decreases rapidly with increasing pump amplitude a_0.

Finally, we study the detuning effect of the nonlinear terms. As indicated in Eq. (10), the nonlinear detuning leads to the nonlinear frequency shift ($B|\bar{f}|^2$), which can stop the three-wave coupling if this frequency shift exceeds the Raman growth rate

$$\frac{12T}{\beta} \omega_f |f|^2 \geq \gamma \;\Rightarrow\; f_{\max}^{\text{nl}} \approx \sqrt{\frac{\gamma\beta}{12T\omega_f}} \sim \frac{\sqrt{a_0}}{\beta^{1/8}} \ll 1. \tag{21}$$

Note that the quantity $12T/\beta$ is of order of unity for typical plasma parameters of an electron temperature of about 15 eV and a plasma density of about 1/100 of critical one. This indicates that the maximum value of density perturbations $f_{\max}^{\text{nl}}$ is still smaller than the background plasma density when $a_0 < \beta^{1/4} \lesssim 1$. Thus, the traditional (kinetic) wavebreaking will never occur under Raman compression with not too large pump amplitudes $a_0 < \beta^{1/4}$ due to the smallness of the Raman growth rate compared to the plasma wave frequency ($\gamma \ll \omega_p$). Inserting Eq. (21) into Eqs. (14) and (16) gives

$$\begin{aligned} b_{\max}^{\text{nl}} &\propto \frac{\beta^{11/8}}{\sqrt{12T}} a_0^{3/2} L = \frac{\beta^{9/8}}{\sqrt{12T}} a_0^{1/2} \Delta, \\ \eta^{\text{nl}} &\propto \frac{\beta^{9/4}}{12 a_0 T} \sim \frac{\beta^{5/4}}{a_0}. \end{aligned} \tag{22}$$

Using the dimensionless normalizations in Eq. (13), the maximum amplified seed amplitude and the efficiency become

$$\bar{b}_{\max}^{\text{nl}} \propto \bar{f}_{\max}^{\text{nl}} \Delta \propto \frac{\Delta}{\sqrt{B}}, \quad \eta^{\text{nl}} \propto \frac{1}{B}. \tag{23}$$

We should note that for the typical plasma utilized in the Raman amplification experiment with $\beta = 0.002 \ldots 0.01$ and pump durations less than tens of picoseconds, the electron temperature will be about the ionization threshold 15…30 eV, i.e., the parameter $12T/\beta$ is among 0.1…1.

According to relation equations (18), (20), and (22), we plot the dependence of the output seed maximum amplitude on the pump amplitude as shown in Fig. 1. The centering vertical dotted line located at the intersection of the blue [Eq. (18)] and green lines [Eq. (20)] defines the traditional wavebreaking criteria [Eq. (1)]

$$a_0 \geq \beta^{3/4}. \tag{24}$$

However, as shown by the red line [Eq. (22)], in the region

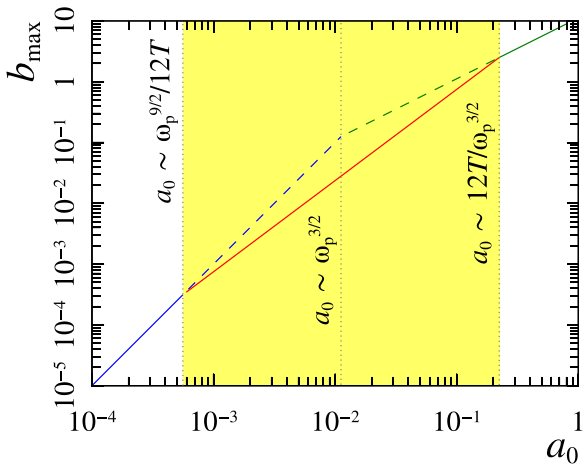

FIG. 1. Typical dependence on maximal output seed amplitude b_{max} depending on pump amplitude a_0. There are 3 segments for formulas Eq. (18) (left, blue), Eq. (22) (middle, red), and Eq. (20) (right, green) respectively. Dots show thresholds between them. Dashed lines show b_{max} according to wavebreaking. The yellow color denotes the region with the nonlinear detuning dominating Eq. (25). This particular figure is plotted for $\omega/\omega_p = 20$ ($\beta = 1/400$) and $T_e = 35$ eV ($T = 0.0002$).

$$\frac{\beta^{9/4}}{12T} \le a_0 \le \frac{12T}{\beta^{3/4}}, \tag{25}$$

the nonlinear detuning effect is dominant, limiting the maximum output seed amplitude below the traditional results. In other words, the nonlinear detuning effect appears at a much smaller pump amplitude threshold than does the wavebreaking one.

From the above simple analysis, several preliminary conclusions can be made. First, Eq. (21) indicates that the fluid dynamic equations are applicable nearly everywhere except in the region where the growth rate is larger than the plasma frequency, which leads to a density fluctuation f_{max}^{nl} that exceeds the background density. Second, in considering the nonlinear detuning effect of plasma waves, the highest amplification efficiency is reachable only for lower pump amplitude ($a_0 \sim \beta^{5/4}$) rather than the wavebreaking threshold ($a_0 \sim \beta^{1/4}$). Moreover, with higher pump amplitude, the efficiency decreases linearly in the pump amplitude ($\eta^{nl} \propto a_0^{-1}$) rather than quadratic in the pump amplitude ($\eta^{wb} \propto a_0^{-2}$).

IV. NUMERICAL SIMULATIONS

We use the kinetic simulations and numerical fluid model simulations to compare with the above analytical predictions. First, we employ the 1D3V particle-in-cell (PIC) code EPOCH[36] to verify our scaling law [Eq. (22)]. In these simulations, 64 cells per wavelength ($\lambda_0 = 0.8\,\mu$m is the pump wavelength) are used with 25 particles per cell. The plasma length is fixed at 4 mm, with an electron number density of $4.4 \times 10^{18}\,\mathrm{cm}^{-3}$ ($\beta = 1/400$). The pump intensity is varied over the range from 10^{14} to $5 \times 10^{15}\,\mathrm{W/cm}^2$, with a constant temporal shape. The seed intensity is fixed at 10^{14} or $10^{15}\,\mathrm{W/cm}^2$, with a temporal Gaussian shape and a FWHM duration of 30 fs. All the parameters are specifically selected to be in the range of Eq. (25) where the detuning

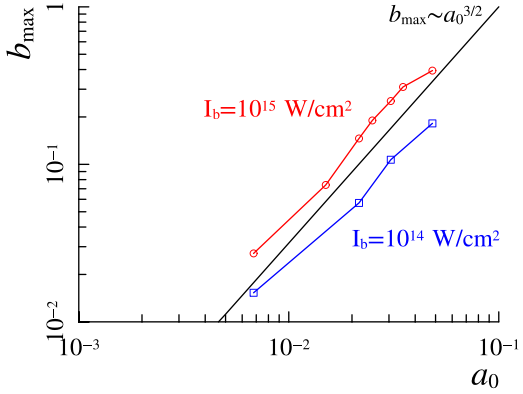

FIG. 2. The result of PIC simulations for maximal seed amplitudes depending on pump amplitude a_0. Simulations were done for different initial seed intensities $I_b = 10^{14}\,\mathrm{W/cm}^2$ and $I_b = 10^{15}\,\mathrm{W/cm}^2$. The straight line is analytical prediction [Eq. (22)].

effect is dominant. The results of the relation of the maximum output seed amplitude with the pump amplitude are shown in Fig. 2, which indicates good agreement with the analytical prediction [Eq. (22)], $b_{max}^{nl} \propto a_0^{3/2} L$, and validates the nonlinear dispersion plasma wave equation [Eq. (10)].

We numerically solve the modified 3-wave equations [Eq. (13)]. Typical output seed structures are shown in Fig. 3(a). They are quite similar to the π-pulse seed solutions but with lower maximum amplitude and much smaller "tail." The larger the detuning effect (larger coefficient B), the lower the maximum amplitude and the smaller the "tail" since the detuned plasma wave limits the energy transfer between the seed and pump in the tail region. The dependence of the maximal plasma wave amplitude and the energy transfer efficiency on the initial seed amplitude and the coefficient B resulting from the numerical simulations are shown in Fig. 4. We see good agreement between the excited plasma wave amplitude and efficiency on one hand and the estimates [Eq. (23)] in the small seed amplitude region ($b_0 < a_0$) on the other hand. However, in the higher seed amplitude cases ($b_0 > a_0$), both the plasma wave amplitude and the amplification efficiency decrease much more slowly with increasing detuning than rates predicted by Eq. (23). This reminds us of the short energetic seed pulse used in the quasitransient regime.[31]

Note that the suppression effect of the nonlinear detuning of the plasma wave can be partially compensated by chirping the pump pulse, i.e., using $a = a_0 \exp(-\mathrm{i}q\gamma^2 t^2)$. Here, q is the chirp coefficient, which was imagined to be in the range $q \approx 0.1 \ldots 0.2$ for the purpose of preventing amplification by noise.[2] The simulations demonstrate that, for not so large a plasma wave detuning ($B \le 100$), a proper pump chirp can delay the phase detuning and lead to higher maximum output seed amplitude. For example, the comparison among Figs. 3(a)–3(e) shows strong output seeds, the intensity of which can even approach that of the ideal π-pulse case shown in Fig. 3(a) and can be obtained for the $B = 30$ and $B = 100$ cases with the pump chirping coefficients $q = 0.3$ and $q = 0.4$, respectively. On the other hand, the pump chirping provides limited improvement in the case of stronger plasma detuning $B \ge 300$, while the pump chirping

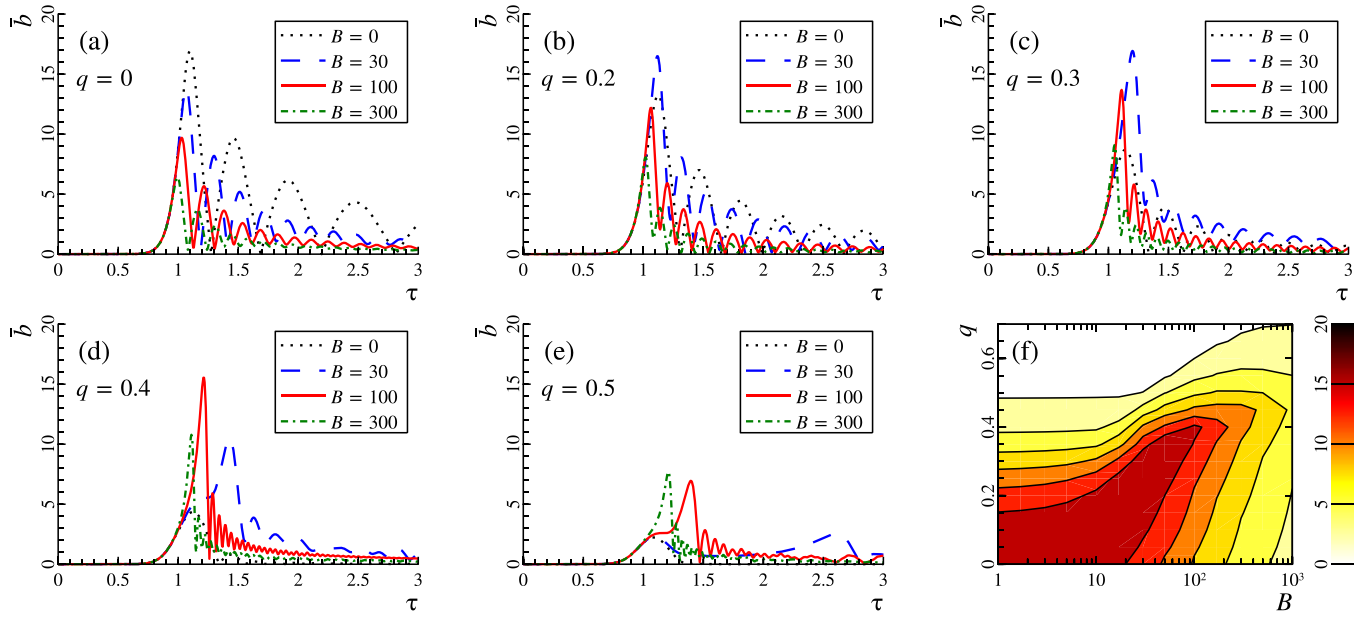

FIG. 3. Typical seed profiles for Eq. (13) for different values of plasma wave detuning coefficient B without (a) and with (b) the chirp of the pump pulse. The initial seed duration is $\gamma\tau_0 = 1/8$, and its amplitude is $b_0/a_0 = 0.1$. Dots show the π-pulse solution ($B = 0$) for the same seed. (f) The dependence of maximum output seed amplitudes on the values of plasma wave detuning coefficient B and pump chirping coefficient q.

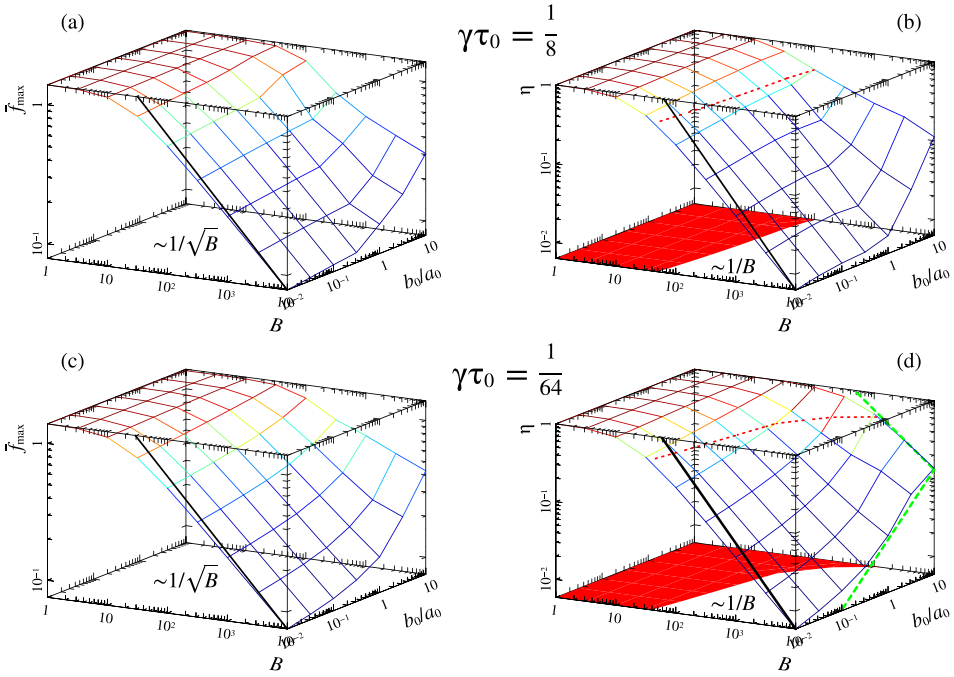

FIG. 4. The maximal plasma wave amplitude and the efficiency depending on initial seed amplitude b_0 and parameter B for different initial seed durations: $\gamma\tau_0 = 1/8$ and $\gamma\tau_0 = 1/64$. Thick lines denote analytical estimation [Eq. (23)]. The filled red area denotes the region where $\eta > 50\%$.

provides little improvement for the stronger plasma detuning $B = 300$ case.

Further detailed parameter scans of the dependence of the output seed amplitude on the plasma wave detuning and pump chirping, as shown in Fig. 3(f), demonstrate that, for stronger nonlinear plasma wave dispersion, the phase detuning is so fast that the further increase in the chirp coefficient q could not compensate it. It can also be observed from Fig. 3(f) that the nonlinear detuning suppresses the output seed intensity when the nonlinear plasma wave dispersion coefficient $B \gtrsim 20$ and the pump chirping is effective for the plasma wave detuning coefficient in the range $20 \lesssim B \lesssim 100$. In addition, the noise scattering is still prevented by the plasma wave detuning $(B|\bar{f}|^2)$ even with the proper pump chirp.

Another simple way of correcting this nonlinear detuning effect is to use a frequency-upshifted pump in the regime when the plasma wave amplitude is large enough and detuning takes place. According to Eq. (21), this nonlinear frequency shift is limited to γ, and thus, by theoretically upshifting the pump frequency $\delta\omega$ with the order of γ in the nonlinear regime where the plasma wave amplitude almost maintains the maximum, the three-wave coupling remains resonant. Here, as an example, using the 1D PIC simulations,

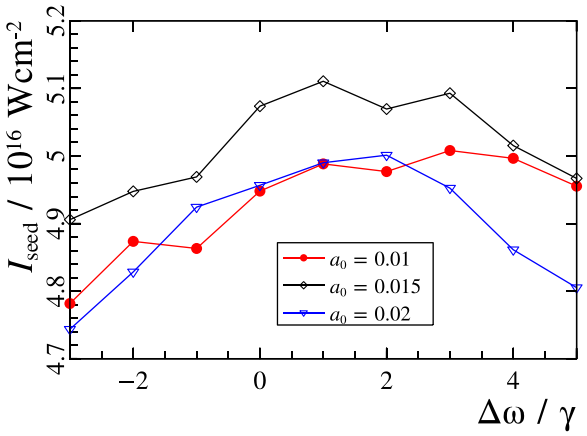

FIG. 5. The output seed intensities in PIC simulations for cases with a secondary pump of different shifted-frequencies. The horizontal axis coordinates denote the frequency shift $\delta\omega$ of the secondary pump normalized by the linear Raman growth rates $\left(\gamma = a_0\sqrt{\beta 4}/\sqrt{2}\right)$. In all simulations, $\beta = 1/400$. The initial seed intensity is 1/10 of the pump intensity. The secondary pump sets in at time t = 4.1 ps, 1.6 ps, and 1.1 ps for $a_0 = 0.01$, 0.015, and 0.02 cases, respectively. The simulation time is 56 ps, 29 ps, and 18 ps for $a_0 = 0.01$, 0.015, and 0.02 cases, respectively.

we compare the intensities of the output seeds amplified by two-pulse-like pumps where the second frequency-shifted-pump pulse sets in at the beginning of the nonlinear regime. The asymmetry of the output seed intensities in cases with frequency-downshifted-pumps and cases with frequency-upshifted-pumps for all the three groups (with pump amplitude $a_0 = 0.01$, 0.015, and 0.02) as shown in Fig. 5 demonstrates the afore-discussed frequency-upshift of the plasma wave caused by the plasma wave dispersion. Meanwhile, we note that the optimum frequency upshift for the secondary pump pulse varies between $\Delta\omega = \gamma \ldots 3\gamma$ for different pump amplitudes.

V. SUMMARY

From first principles, we derived the modified Raman 3-wave interaction equations, taking into account the influence of nonlinear dispersion of the plasma wave. It is found that, in certain regimes, rather than wavebreaking, the dominant effect of the nonlinear dispersion is nonlinear detuning, which appears as a simple cubic nonlinearity [see Eq. (10)]. In the process of Raman compression, this nonlinear detuning can limit the plasma wave to amplitudes noticeably below the wavebreaking threshold. The estimates of the maximum output seed amplitude and Raman compression efficiency, taking into account plasma wave detuning, are obtained for low seed amplitude $b_0 \ll a_0$. The kinetic PIC simulation results confirm these simple estimations. We also numerically demonstrate that proper pump chirping or, equivalently, pump-frequency-upshift in the nonlinear stage helps to counteract this nonlinear detuning effect.

ACKNOWLEDGMENTS

We are grateful to the referee for valuable comments.

This research was supported by AFOSR under Grant No. FA9550-15-1-0391. A. A. Balakin is grateful to the Russian Science Foundation (Project No. 17-72-20111) for supporting the research carried out in Sec. II.

[1]V. M. Malkin, G. Shvets, and N. J. Fisch, Phys. Rev. Lett. **82**, 4448 (1999).
[2]V. M. Malkin, G. Shvets, and N. J. Fisch, Phys. Plasmas **7**, 2232 (2000).
[3]N. J. Fisch and V. M. Malkin, Phys. Plasmas **10**, 2056 (2003).
[4]Y. Ping, W. Cheng, S. Suckewer, D. S. Clark, and N. J. Fisch, Phys. Rev. Lett. **92**, 175007 (2004).
[5]A. A. Balakin, D. V. Kartashov, A. M. Kiselev, S. A. Skobelev, A. N. Stepanov, and G. M. Fraiman, Pisma Zh. Eksp. Teor. Fiz. **80**, 15 (2004) [JETP Lett. **80**, 12 (2004)].
[6]W. Cheng, Y. Avitzour, Y. Ping, S. Suckewer, N. J. Fisch, M. S. Hur, and J. S. Wurtele, Phys. Rev. Lett. **94**, 045003 (2005).
[7]A. A. Balakin, G. M. Fraiman, N. J. Fisch, and S. Suckewer, Phys. Rev. E **72**, 036401 (2005).
[8]R. K. Kirkwood, E. Dewald, C. Niemann, N. Meezan, S. C. Wilks, D. W. Price, O. L. Landen, J. Wurtele, A. E. Charman, R. Lindberg, N. J. Fisch, V. M. Malkin, and E. O. Valeo, Phys. Plasmas **14**, 113109 (2007).
[9]J. Ren, S. Li, A. Morozov, S. Suckewer, N. A. Yampolsky, V. M. Malkin, and N. J. Fisch, Phys. Plasmas **15**, 056702 (2008).
[10]R. L. Berger, D. S. Clark, A. A. Solodov, E. J. Valeo, and N. J. Fisch, Phys. Plasmas **11**, 1931 (2004).
[11]Y. A. Tsidulko, V. M. Malkin, and N. J. Fisch, Phys. Rev. Lett. **88**, 235004 (2002).
[12]V. M. Malkin, Y. A. Tsidulko, and N. J. Fisch, Phys. Rev. Lett. **85**, 4068 (2000).
[13]V. M. Malkin, Z. Toroker, and N. J. Fisch, Phys. Rev. E **90**, 063110 (2014).
[14]G. Lehmann and K. Spatschek, Phys. Plasmas **21**, 053101 (2014).
[15]I. Barth, Z. Toroker, A. A. Balakin, and N. J. Fisch, Phys. Rev. E **93**, 063210 (2016).
[16]V. M. Malkin and N. J. Fisch, Phys. Rev. Lett. **117**, 133901 (2016).
[17]V. M. Malkin, G. Shvets, and N. J. Fisch, Phys. Rev. Lett. **84**, 1208 (2000).
[18]Z. Toroker, V. M. Malkin, and N. J. Fisch, Phys. Rev. Lett. **109**, 085003 (2012).
[19]M. S. Hur, D. N. Gupta, and H. Suk, J. Phys. D: Appl. Phys. **40**, 5155 (2007).
[20]G. Vieux, A. Lyachev, X. Yang, B. Ersfeld, J. P. Farmer, E. Brunetti, R. C. Issac, G. Raj, G. H. Welsh, S. M. Wiggins, and D. A. Jaroszynski, New J. Phys. **13**, 063042 (2011).
[21]R. Nuter and V. Tikhonchuk, Phys. Rev. E **87**, 043109 (2013).
[22]X. Yang, G. Vieux, E. Brunetti, B. Ersfeld, J. P. Farmer, M. S. Hur, R. C. Issac, G. Raj, S. M. Wiggins, G. H. Welsh, S. R. Yoffe, and D. A. Jaroszynski, Sci. Rep. **5**, 13333 (2015).
[23]A. A. Balakin, I. Y. Dodin, G. M. Fraiman, and N. J. Fisch, Phys. Plasmas **23**, 083115 (2016).
[24]Z. Mahdian, S. Mirzanejhad, T. Mohsenpour, and M. Taghipour, Optik **149**, 372 (2017).
[25]N. A. Yampolsky, N. J. Fisch, V. M. Malkin, E. J. Valeo, R. Lindberg, J. S. Wurtele, J. Ren, S. Li, A. Morozov, and S. Suckewer, Phys. Plasmas **15**, 113104 (2008).
[26]N. A. Yampolsky and N. J. Fisch, Phys. Plasmas **18**, 056711 (2011).
[27]Z. Toroker, V. M. Malkin, and N. J. Fisch, Phys. Plasmas **21**, 113110 (2014).
[28]M. R. Edwards, Z. Toroker, J. M. Mikhailova, and N. J. Fisch, Phys. Plasmas **22**, 074501 (2015).
[29]J. P. Farmer and A. Pukhov, Phys. Rev. E **92**, 063109 (2015).
[30]R. M. G. M. Trines, F. Fiuza, R. Bingham, R. A. Fonseca, L. O. Silva, R. A. Cairns, and P. A. Norreys, Nat. Phys. **7**, 87 (2011).
[31]V. M. Malkin and N. J. Fisch, Phys. Rev. E **80**, 046409 (2009).
[32]A. A. Balakin, N. J. Fisch, G. M. Fraiman, V. M. Malkin, and Z. Toroker, Phys. Plasmas **18**, 102311 (2011).
[33]C. J. McKinstrie, A. Simon, and E. A. Williams, Phys. Fluids **27**, 2738 (1984).
[34]O. Yaakobi, L. Friedland, R. R. Lindberg, A. E. Charman, G. Penn, and J. S. Wurtele, Phys. Plasmas **15**, 032105 (2008).
[35]P. Khain, L. Friedland, A. G. Shagalov, and J. S. Wurtele, Phys. Plasmas **19**, 072319 (2012).
[36]T. D. Arber, K. Bennett, C. S. Brady, A. Lawrence-Douglas, M. G. Ramsay, N. J. Sircombe, P. Gillies, R. G. Evans, H. Schmitz, A. R. Bell, and C. P. Ridgers, Plasma Phys. Controlled Fusion **57**, 113001 (2015).